

# Basaltic Shergottite NORTHWEST AFRICA 856: Differentiation of a Martian Magma



J. Ferdous<sup>1</sup>, A. D. Brandon<sup>1</sup>, A. H. Peslier<sup>2</sup> and Z. Pirotte<sup>3</sup>

<sup>1</sup>University of Houston, Houston TX 77204, USA, jferdous@uh.edu, <sup>2</sup>Jacobs, NASA-Johnson Space Center, Mail Code X13, Houston TX 77058, USA, <sup>3</sup>Dept. de Géologie, Université Libre de Bruxelles, 1050 Brussels, Belgium.



## Introduction

**NWA 856:** (Djel Ibone)

- Basaltic shergottite
- Discovered in South Morocco in April, 2001 [1]
- Found as single stone of 320 gm [1]
- Fresh, fine grained
- Covered with thin black-fusion crust
- Highly fractured
- Terrestrially less weathered as a desert find [1]
- Crystallization age: 150 ± 32 Ma (Rb-Sr isotope system) and 186 ± 24 Ma (Sm-Nd isotope system) [2]
- Bulk rock oxygen isotope:  $\delta^{17}\text{O} = +3.09\text{‰}$ ,  $\delta^{18}\text{O} = +5.03\text{‰}$ ,  $\Delta^{17}\text{O} = +0.47\text{‰}$  [1]



**Figure 1:** NWA 856 showing thin fusion crust and interior basaltic texture. (Photo Courtesy: Bruno Fectay and Carine Bidant)

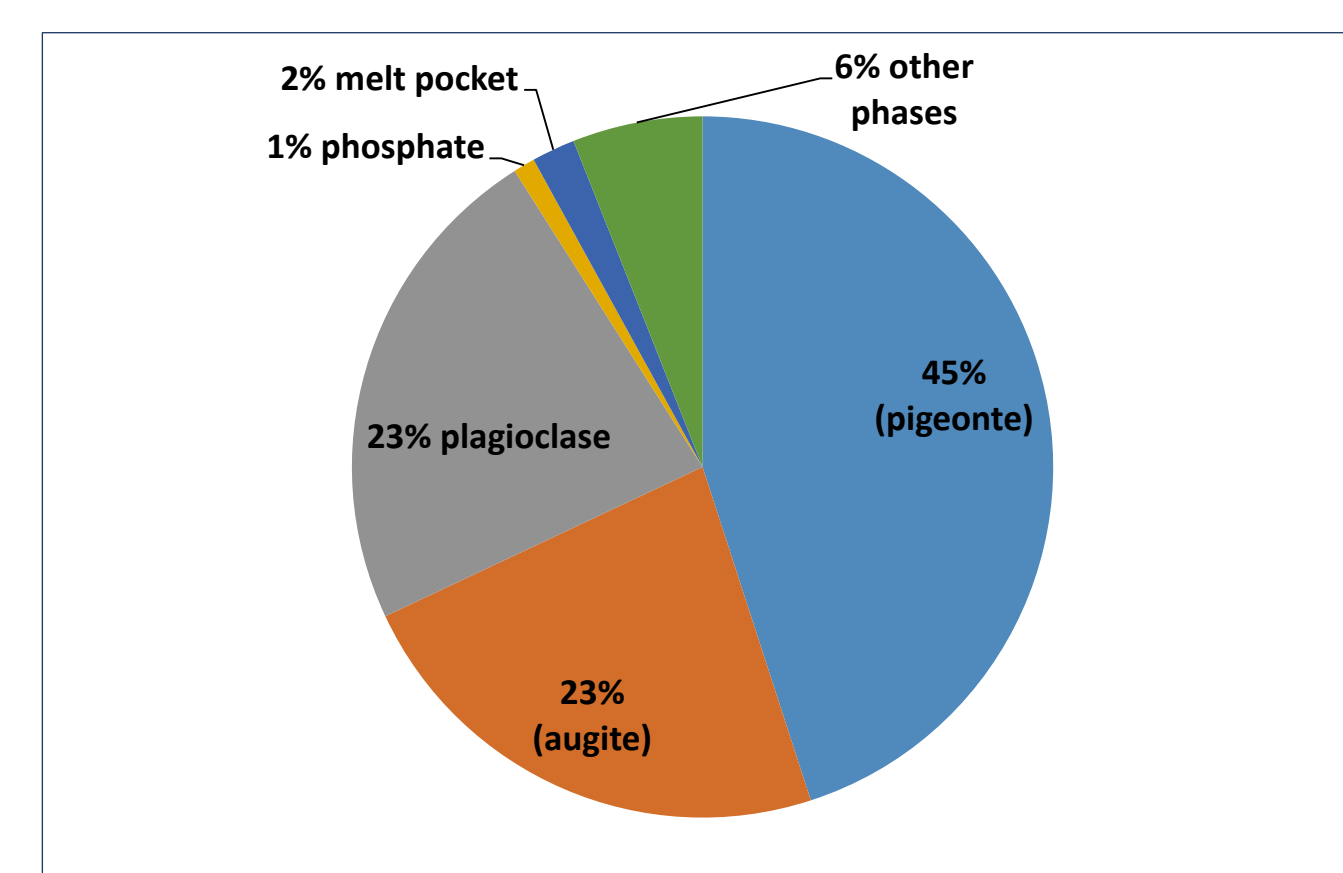


**Figure 2:** Major phases and modal abundances of NWA 856 [1].

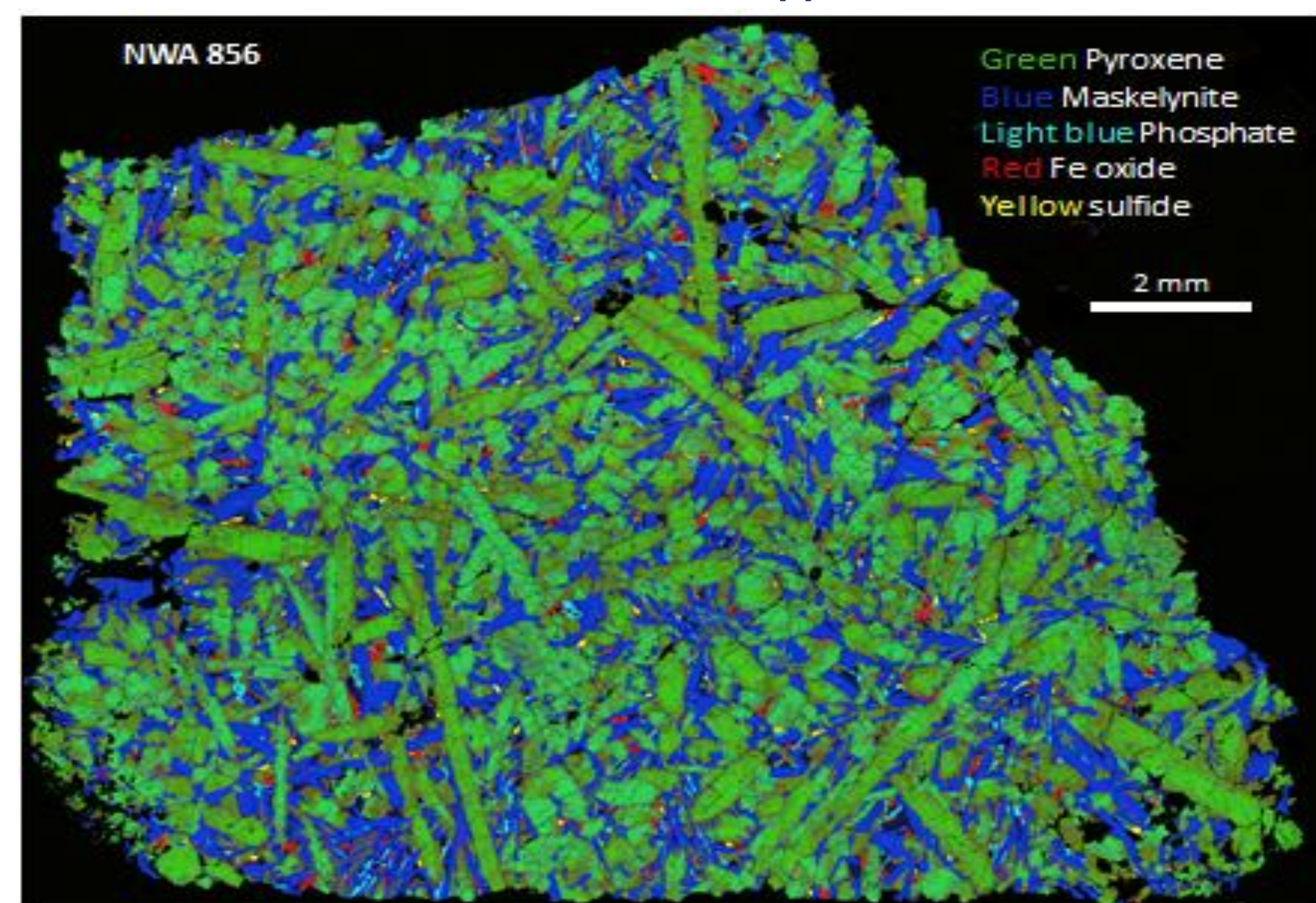


**Figure 3:** Multi-element (Si, Mg, Fe, Ca, Ni, S) map of NWA 856 obtained from Energy Dispersive X-ray (EDX) analysis.

## Objective

The purpose of this study is to constrain the crystallization history of NWA 856 using textural observations, crystallization sequence modeling and in-situ trace element analysis in order to understand differentiation in shergottite magmatic systems.

## Analytical Techniques

A polished thick section (15 x 13 x 2 mm) was used for EDX-elemental mapping by scanning electron microscope (SEM JEOL 7600F). An electron microprobe (EMP) Cameca SX100 was used to obtain in situ major element concentrations of each phase. Both instruments are located in the ARES division of NASA-Johnson Space Center.

Major, minor and trace element abundances in minerals were measured using a Varian 810 inductively coupled plasma mass spectrometer connected to a CETAC LSX-213 laser ablation system (LA-ICP-MS) in the department of Earth and Atmospheric Sciences of the University of Houston. The sizes of the analyzed spots were 20-100  $\mu\text{m}$  in diameter. The software GLITTER was used to calculate concentrations. Analyses were normalized to CaO contents obtained from EMP analyses. Basalt glass BHVO-2G (USGS standard) was used for calibration while BIR-1G (USGS standard) was used as an external standard to monitor accuracy and reproducibility.

## Mineralogy

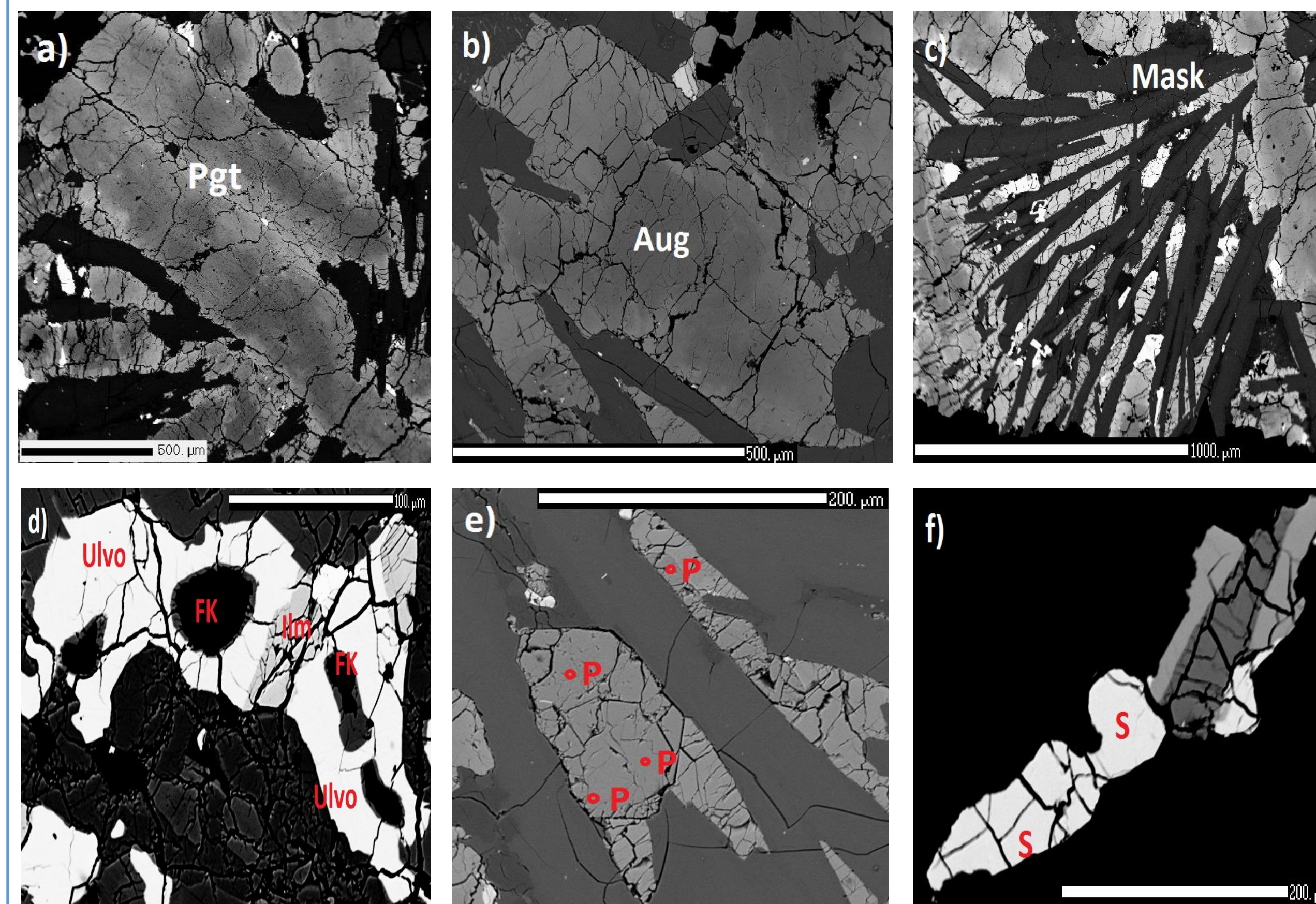


**Figure 4:** BSE-images of different mineral phases: major phases a) zoned pigeonite (Pgt) b) zoned augite (Aug) c) maskelynite (Mask) and minor phases d) ulvöspinel (Ulvo), ilmenite (Ilm) and amorphous K-feldspar (FK) e) phosphates (P) f) sulfides (S).

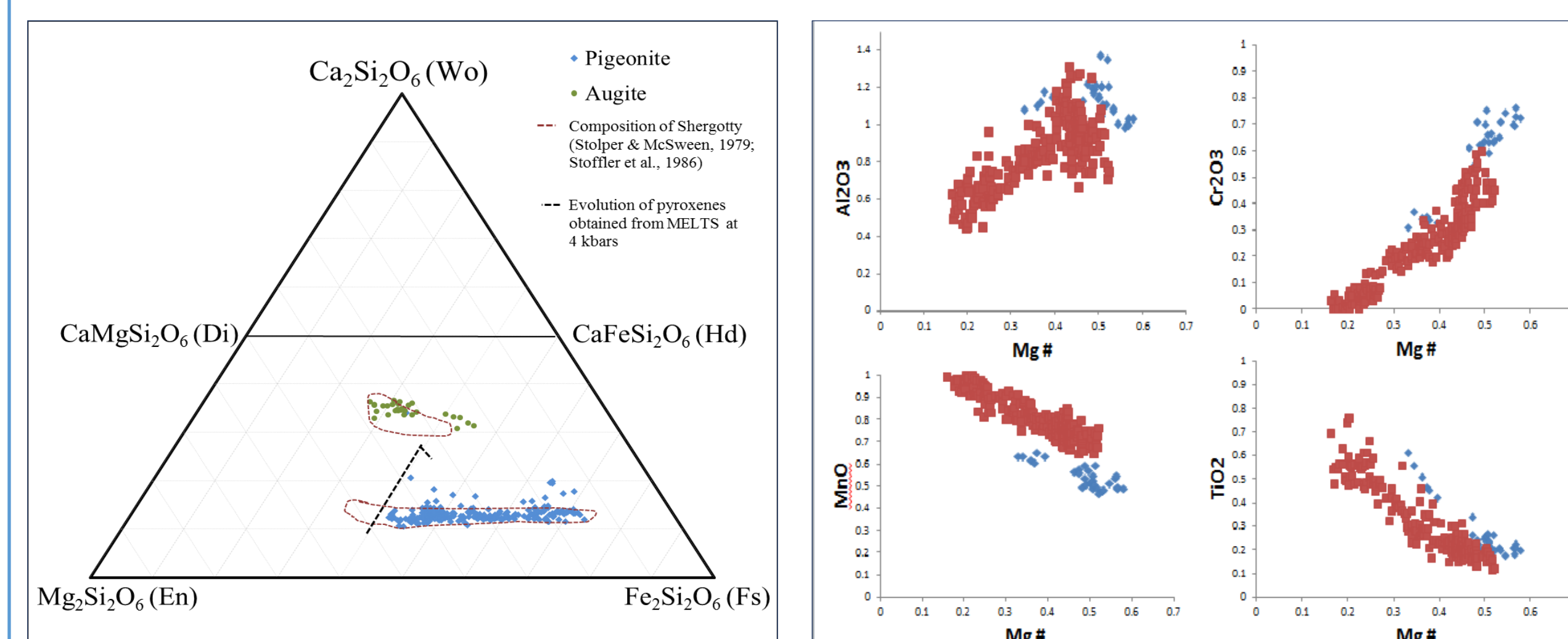


**Figure 5:** Triangular diagram of pyroxene compositions of NWA 856 compared to Shergotty and compositional evolution of NWA 856 obtained from MELTS.

**Figure 6:** Range of minor element compositions versus Mg# ( $\text{Mg}/(\text{Mg}+\text{SFe}^{2+})$ ) in pyroxenes of NWA 856. All oxides are in wt%. Here, red squares are pigeonites and blue diamonds are augites.

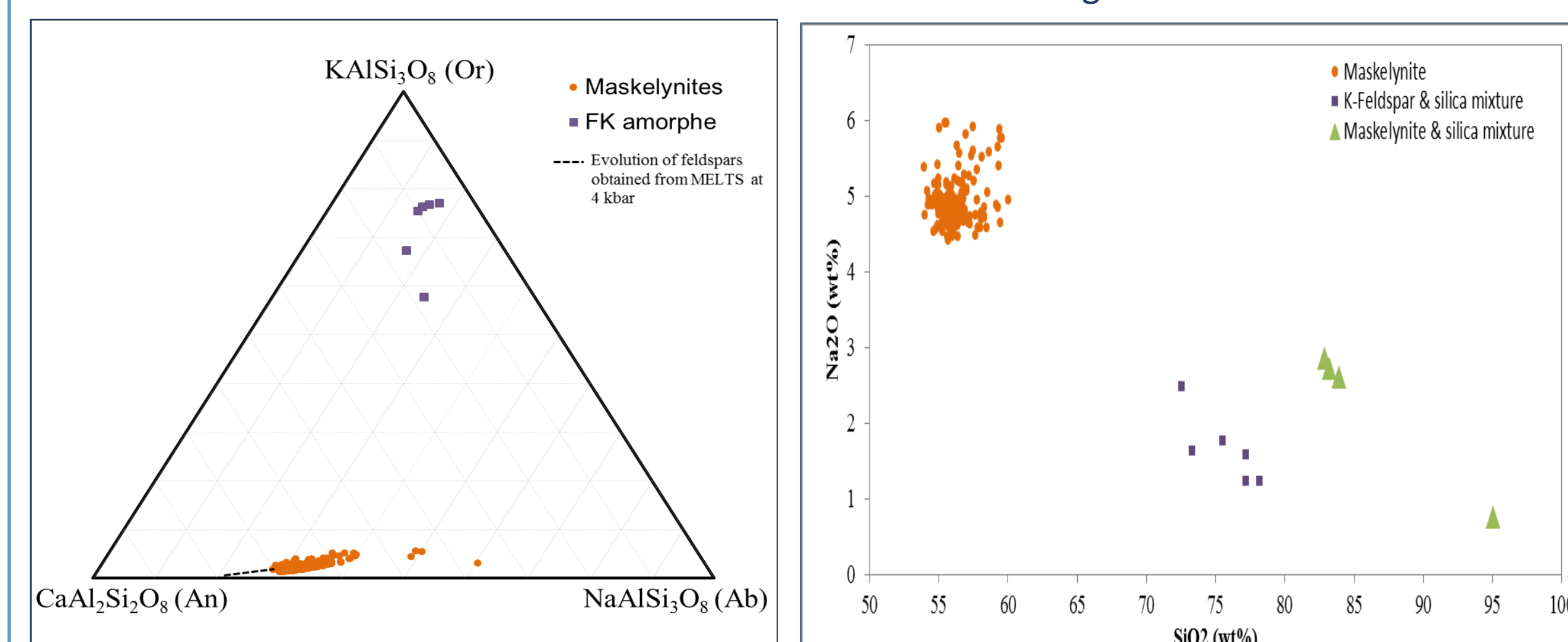


**Figure 7:** Triangular plotting of the feldspar compositions of NWA 856 with compositional evolution obtained from MELTS.

**Figure 8:** Maskelynite compositions show localized Si-enrichment indicating contribution from evolved phases such as K-feldspar and  $\text{SiO}_2$ .

## Shock Features

- Highly fractured
- Maskelynitization
- Pyroxene dislocations and twins [3]
- Abundant impact melt pockets [4]
- Presence of stishovite and high silica glass [1, 4]

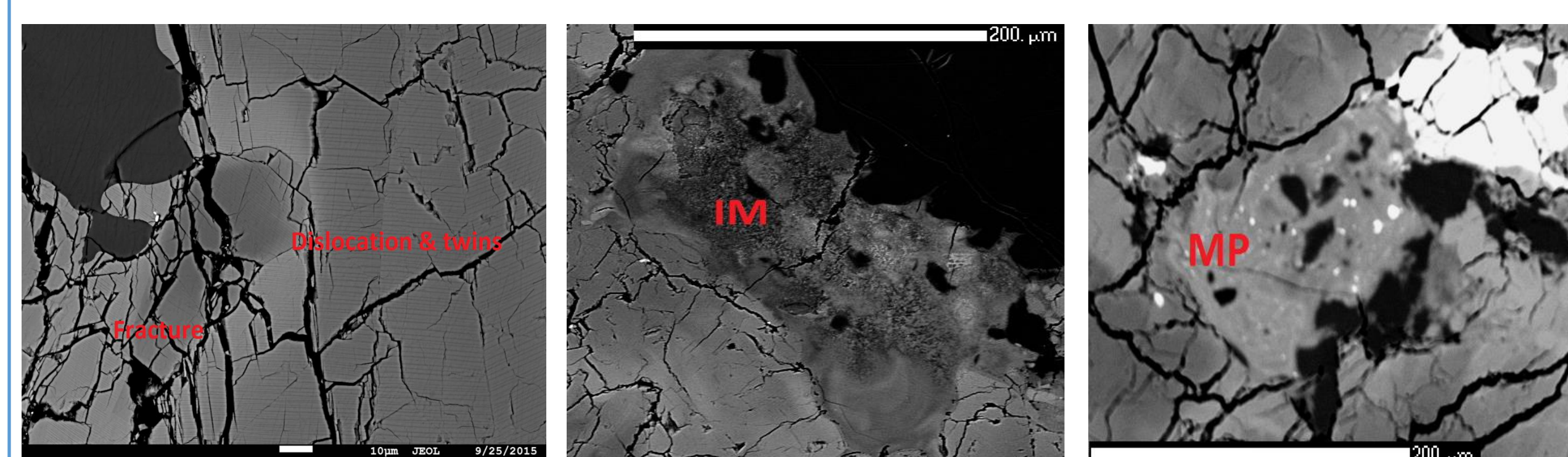


**Figure 9:** Shock features of NWA 856: pyroxene dislocation and twins, shocked impact melt (IM) and late stage crystallized melt pocket (MP) (from left to right).

## Crystallization Sequence

The crystallization sequence of NWA 856 is derived from textural relationships and compared to results from MELTS simulations [5] using NWA 856 bulk composition from [1] as initial composition. MELTS simulation, result in the same crystallization sequences at 4 kbar and 5 kbar and those run under fractionation conditions are most consistent with our textural analysis.

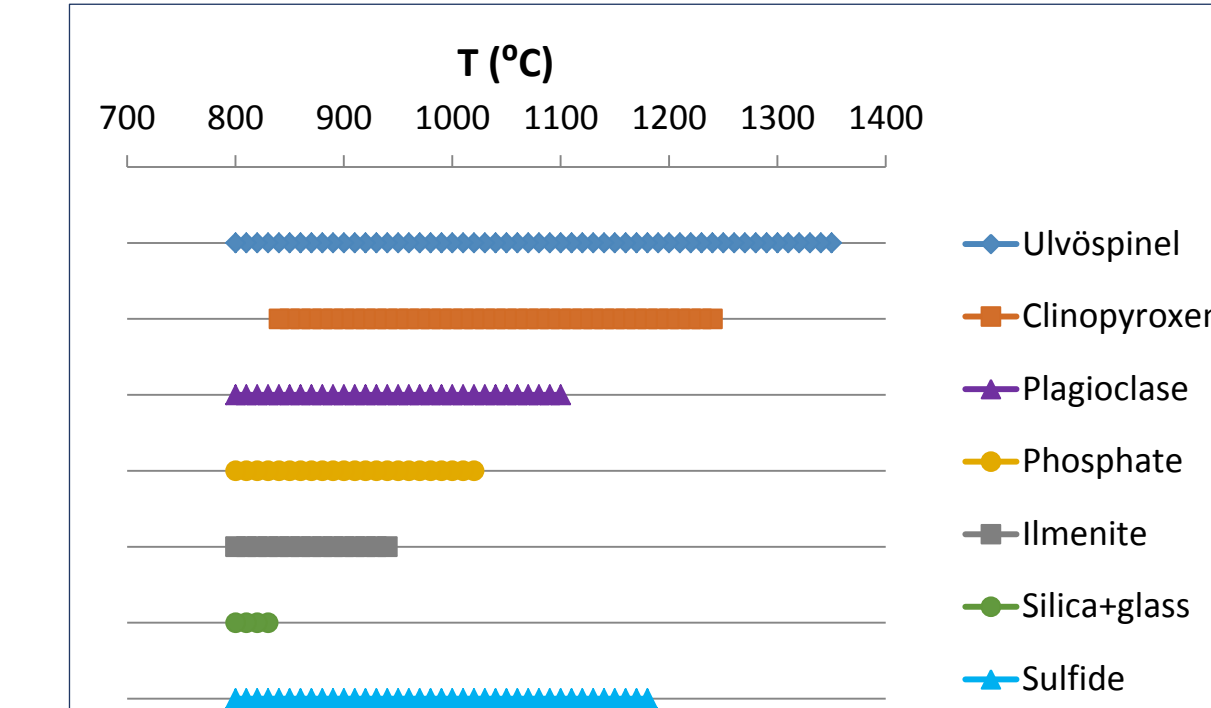


**Figure 10:** Crystallization sequence based on textural and compositional observations.

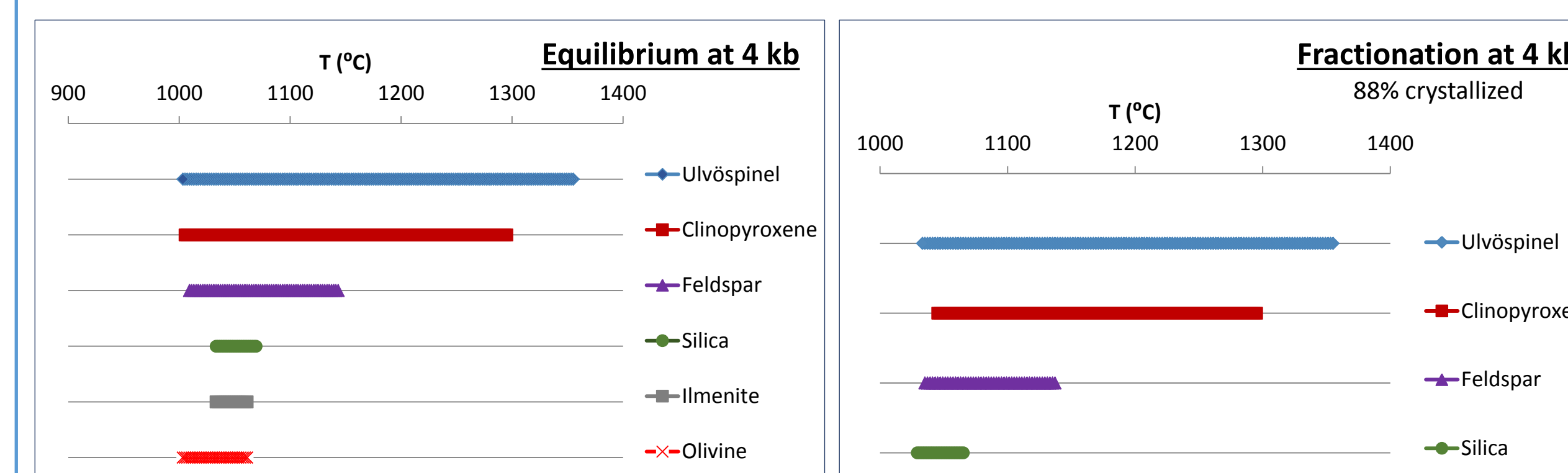


**Figure 11:** Crystallization sequence based on MELTS simulation of isobaric equilibrium and fractional crystallization.

## In-Situ Trace-Elements

NWA 856 is an enriched basaltic shergottite with flat rare earth element (REE)-pattern similar to Shergotty and Zagami [1]. The absence of positive Ce-anomalies and lower contents of Cs, Ba and Sr in all phases when compared to other desert finds indicate that NWA 856 is the least affected by terrestrial weathering and alteration.

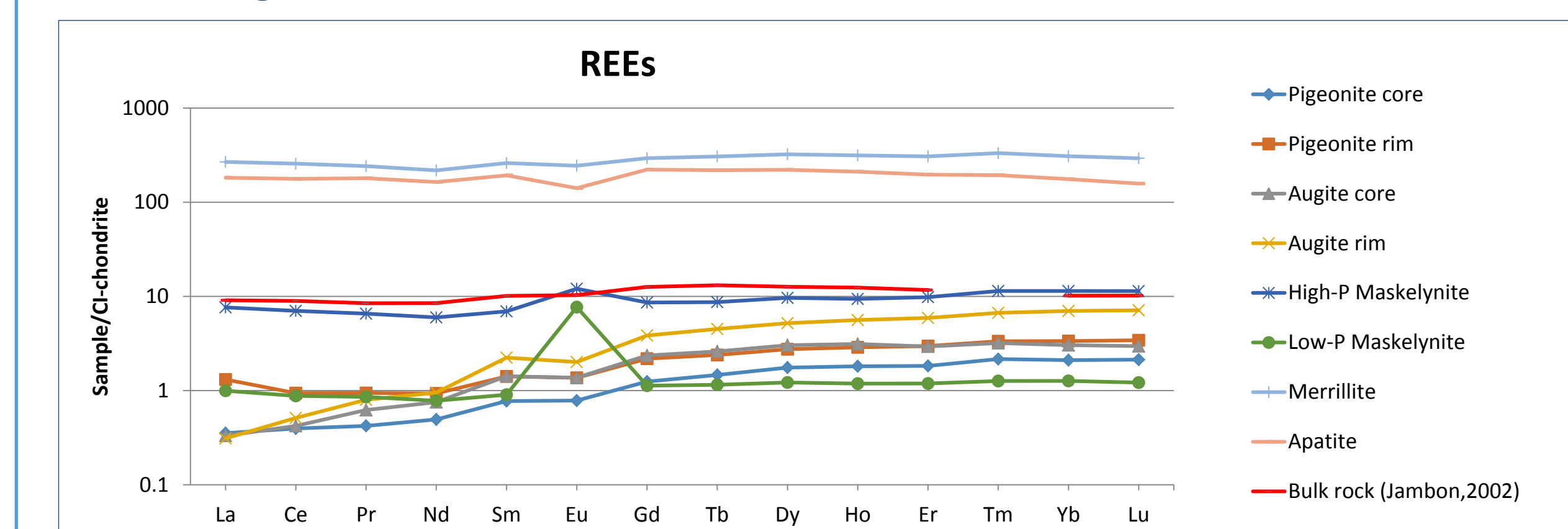


**Figure 12:** Cl-chondrite normalized measured REE-patterns of zoned clinopyroxenes, maskelynites, phosphates and bulk composition.

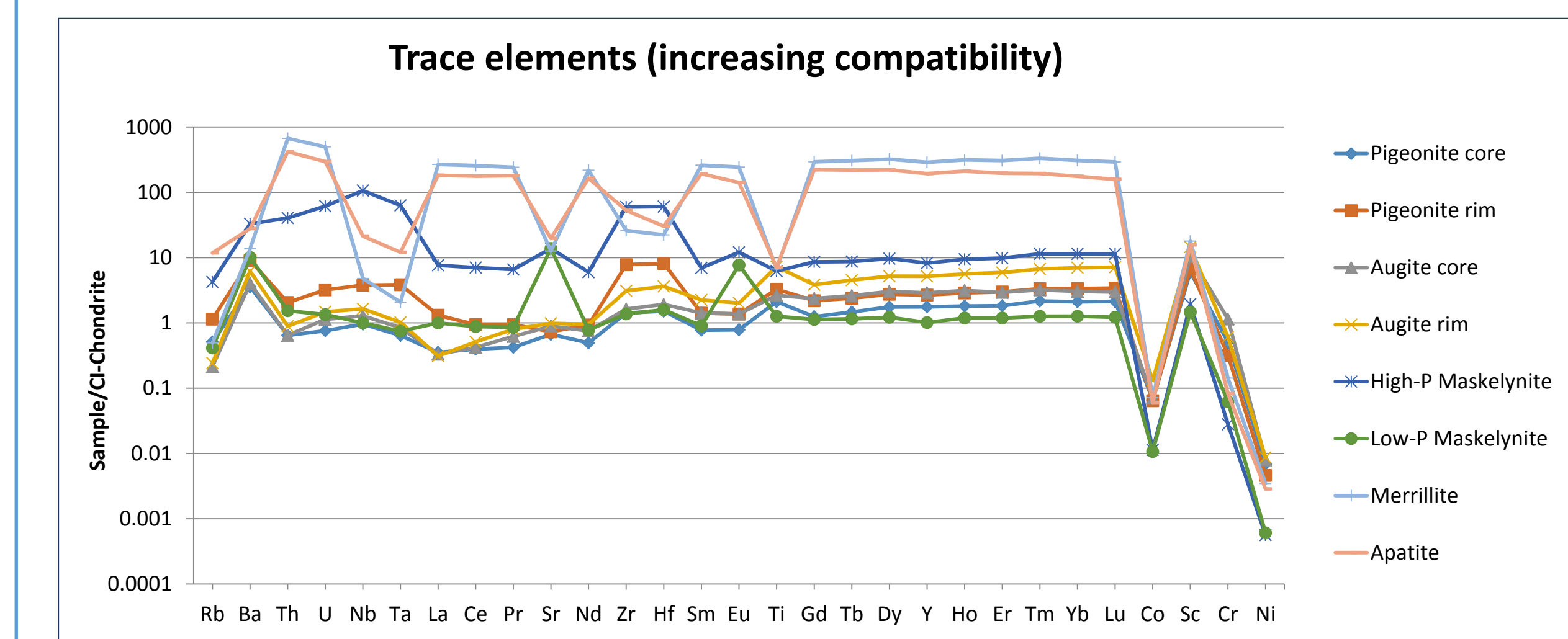


**Figure 13:** Cl-chondrite normalized REEs, LILE, HFSE and transitional metals of zoned clinopyroxenes, maskelynites, phosphates with increasing compatibility from left to right.

## Discussion and Conclusion

The results of petrography, EMP, LA-ICP-MS analyses and MELTS simulations are consistent with the findings of [1]. Pyroxene and spinel began to crystallize first. This was followed by a multistage crystallization sequence with plagioclase formation and final crystallization of phosphates and ilmenite. Pyroxene cores are not disturbed by alteration or shock but plagioclase was shocked into maskelynite with local incorporation of phosphates. NWA 856 closely resembles Shergotty and Zagami, but the lack of mesostasis, larger grain size, an abundance of impact melt pockets and minimal terrestrial weathering separate NWA 856 from any other basaltic shergottites.

## References

- Jambon et al. (2002), *MAPS*, 37, 1147-1164.
- Brandon et al. (2004), *LPSC XXXV*, #1931.
- Leroux et al. (2004), *MAPS*, 39, 711-722.
- Leroux and Cordier (2006), *MAPS*, 41, 913-923.
- Asimow and Ghiorso (1998), *AM*, 83, 1127-1131.